THE JOURNAL OF BIOLOGICAL CHEMISTRY
Vol. 277, No. 34, Issue of August 23, pp. 30436–30444, 2002
Printed in U.S.A.

Structural Basis and Mechanism of the Inhibition of the Type-3 Copper Protein Tyrosinase from *Streptomyces antibioticus* by Halide Ions*

Received for publication, March 14, 2002, and in revised form, May 3, 2002
Published, JBC Papers in Press, June 4, 2002, DOI 10.1074/jbc.M202461200

Armand W. J. W. Tepper‡, Luigi Bubacco§, and Gerard W. Canters‡¶

From the ‡Leiden institute of Chemistry, Gorlaeus Laboratories, Leiden University, Einsteinweg 55, 2333 CC Leiden, The Netherlands and the §Department of Biology, University of Padua, Via Trieste 75, 30121 Padua, Italy

The inhibition of the type-3 copper enzyme tyrosinase by halide ions was studied by kinetic and paramagnetic ^{1}H NMR methods. All halides are inhibitors in the conversion of L-3,4-dihydroxyphenylalanine (L-DOPA) with apparent inhibition constants that follow the order $I^- < F^- \ll Cl^- < Br^-$ at pH 6.80. The results show that the inhibition arises from the interaction of halide with both the oxidized (affinity $F^- > Cl^- > Br^- \gg I^-$) and reduced (affinity $I^- > Br^- > Cl^- \gg F^-$) enzyme. The paramagnetic ^{1}H NMR of the oxidized enzyme complexed with the halides is consistent with a direct interaction of halide with the type-3 site and shows that the $(Cu\text{-}His_3)_2$ coordination occurs in all halide-bound species. It is surmised that halides bridge both of the copper ions in the active site. Fluoride and chloride are shown to bind only to the low pH form of oxidized tyrosinase, explaining the strong pH dependence of the inhibition by these ions. We further show that *p*-toluic acid and the bidentate transition state analogue, Kojic acid, displace chloride from the oxidized active site, whereas the monodentate substrate analogue, *p*-nitrophenol, forms a ternary complex with the enzyme and the chloride ion. On the basis of the experimental results, a model is formulated for the inhibitor action and for the reaction of diphenols with the oxidized enzyme.

One of the unresolved questions in the enzymology of the type-3 copper-containing tyrosinases (EC 1.14.18.1) is the detailed molecular mechanism of both inhibitor action and substrate conversion. This report focuses on the mechanism of their inhibition by halides. Tyrosinases are monooxygenating enzymes catalyzing the *ortho*-hydroxylation of monophenols and the subsequent oxidation of the diphenolic products to the corresponding quinones. The reactions take place under concomitant reduction of molecular oxygen to water. The formed quinones are reactive precursors in the synthesis of melanin pigments. In fruits, vegetables, and mushrooms, Ty[1] is a key enzyme in the browning that occurs upon bruising or long-term storage. In mammals, Ty is responsible for skin pigmentation. Defects in the enzyme may lead to some forms of oculocutaneous albinism or vitiligo (1). Furthermore, the enzyme has been linked to Parkinson's and other neurodegenerative diseases (2–6). Consequently, the enzyme poses considerable interest from medical, agricultural, and industrial points of view.

The current knowledge of Ty at the biological, mechanistic, and structural levels has recently been reviewed (7–10). Ty harbors a dinuclear so-called type-3 copper center, the occurrence of which has also been established in hemocyanins, which act as oxygen carriers in arthropods and mollusks, and the catechol oxidases, which oxidize *o*-diphenols to the corresponding quinones. The two closely spaced copper ions in the type-3 active site are coordinated each by 3 histidine residues through the Nϵ nitrogen atoms (9). Although the known type-3 centers are found to be similar both in structure and in their ability to bind molecular oxygen, they perform different functions. These differences are believed to result from variations in the substrate binding pocket or the accessibility of substrates to the active site, although the exact reasons remain to be defined (7).

The reduced species (Ty_{red}; [Cu(I) (CuI)], binds oxygen to render (*b*) the oxygenated form (Ty_{oxy}; [Cu(II)-O_2^{2-}-Cu(II)]. In Ty_{oxy}, molecular oxygen is bound as peroxide in a μ-η^2:η^2 side-on bridging mode, which destabilizes the O-O bond and activates it for reaction with mono- or diphenols (9). The Ty_{oxy} species shows a strong LMCT (ligand to metal charge transfer transition) at ~345 nm ($\epsilon \approx 18.5\ mM^{-1}cm^{-1}$) and is EPR silent. The latter property also holds for (*c*) the resting form of the enzyme, *i.e.* the oxidized derivative (Ty_{met}; [Cu(II)-Cu(II)] where antiferromagnetic coupling between the unpaired spins of the Cu^{2+} ions occurs through spin super-exchange mediated by a Cu_2 bridging ligand (11). Because of the diamagnetic nature of both Ty_{oxy} and Ty_{met} in the ground state, magnetic resonance studies on Ty and its inhibitor bound species until now mainly dealt with (*d*) the EPR active half-reduced species ($Ty_{half\text{-}met}$; [Cu(I) Cu(II)]), which can be prepared by partial reduction of Ty_{met} (12). Albeit a nonphysiological derivative, EPR studies on $Ty_{half\text{-}met}$ have yielded a considerable amount of information on the structure of the active site and its ligand-bound derivatives (12, 13). The various species discussed above, with the exception of $Ty_{half\text{-}met}$, fit into a reaction cycle that is represented by Scheme 1.

Recently, we have shown that the oxidized enzyme, Ty_{met}, is

* This work was performed under the auspices of the Graduate Research School "Structure and Function of Biomacromolecules (BIOMAC)" of Leiden and Delft Universities and was supported by the Netherlands Foundation for Chemical Research (SON) with financial aid from the Netherlands Organization for Scientific Research (NWO). The costs of publication of this article were defrayed in part by the payment of page charges. This article must therefore be hereby marked "*advertisement*" in accordance with 18 U.S.C. Section 1734 solely to indicate this fact.

[S] The on-line version of this article (available at *http://www.jbc.org*) contains Supplemental Material, a figure showing inhibition data for all halides.

¶ To whom correspondence should be addressed: Leiden University, Einsteinweg 55, P.O. Box 9502, 2300 RA Leiden, The Netherlands. Tel.: 31-71-527-4256; Fax: 31-71-527-4349; E-mail: canters@chem.leidenuniv.nl; Internet: wwwchem.leidenuniv.nl/metprot.

[1] The abbreviations used are: Ty, tyrosinase; L-DOPA, L-3,4-dihydroxyphenylalanine; NOE, nuclear Overhauser effect; LMCT (ligand to metal charge transfer transition; WEFT, water-suppressed equilibrium Fourier transform; FID, free induction decay.

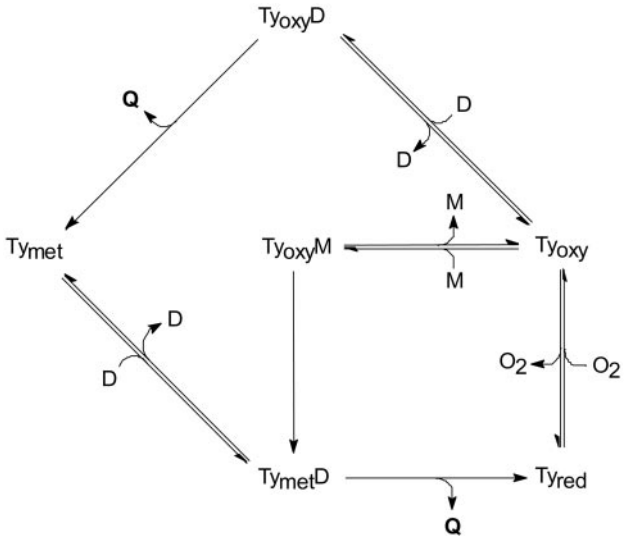

SCHEME 1. **The Ty reaction cycle (9).** *M*, monophenol; *D*, diphenol; *Q*, quinone product. The nomenclature of the Ty species is that used in the text.

amenable to paramagnetic NMR spectroscopy (14, 15). Although the Cu(II)-Cu(II) ground state is a diamagnetic $S = 0$ singlet, the paramagnetic $S = 1$ triplet state appears to be populated at room temperature, providing sufficient paramagnetism for the signals originating from nuclei of the coordinated His residues and from exogenous ligands to shift outside the diamagnetic envelope, thereby providing a detailed fingerprint of the active site. Especially in the presence of chloride, ^{1}H NMR resonances appear remarkably sharp for a Cu(II) system, by virtue of which it was possible to show that Ty contains a classical type-3 copper site as found in hemocyanins and catechol oxidases (14). The ^{1}H paramagnetic NMR spectrum furthermore drastically changes when competitive inhibitors that mimic the transition state are bound to the active site (15).

The inhibition of Ty by halides has already been reported a long time ago (16–18) but, despite the universal presence of chloride in biological systems ([Cl^-] 5–200 mM), it has never been addressed in kinetic and/or structural detail. The current knowledge concerning Ty halide inhibition is mainly limited to the observations that the inhibition is strongly pH-dependent and that the order of inhibition strength of F^-, Cl^-, Br^-, and I^- appears to be dependent on the source of the enzyme studied (16–18). The latter differences have been explained mainly in terms of the accessibility of the halide ion to the Ty active site (17). Furthermore, EPR studies on halide-bound half-met hemocyanin derivatives have been reported (11, 19), showing that halides interact directly with copper in the type-3 hemocyanin active site.

Here we report on a detailed study of the inhibition of the 31-kDa Ty from *Streptomyces antibioticus* by halide ions, using paramagnetic ^{1}H NMR as a complementary technique to the more conventional kinetic and optical spectroscopic methods. The pH dependence of halide inhibition in the conversion of L-DOPA and of halide binding to Ty_{met} were studied, providing insight into the halide inhibition at a structural and at a mechanistic level and resulting in the proposal of a halide binding mode. Our results address for the first time the Ty halide inhibition by considering the interaction of halide with the physiologically relevant Ty species that participate in the enzymatic reaction pathway. The results show that the halide inhibition derives from the interaction of halide with the Cu_2 center of both the oxidized and the reduced Ty species, where the halide binding affinity is found to be dependent on the nature of the halide ion as well as on the Ty oxidation state. Furthermore, we show that halides can be used as probes in paramagnetic ^{1}H NMR investigations of the coordination mode of exogenously added ligands such as substrate and transition-state analogues as well as aromatic carboxylic acid inhibitors. The relevance of the findings toward understanding the reaction of diphenolic substrates with Ty_{met} is discussed, forming the basis of a proposed structural scheme of Ty inhibition and of the reaction of Ty_{met} with diphenolic substrates.

EXPERIMENTAL PROCEDURES

Protein Isolation and Purification—The enzyme was obtained from the growth medium of liquid cultures of *S. antibioticus* harboring the pIJ703 Ty expression plasmid (15). The protein was purified according to published procedures (15). Purity was checked by SDS-PAGE and exceeded 95% in all preparations. Protein concentrations in pure samples were routinely determined optically using a value of 82 $mM^{-1}cm^{-1}$ for the extinction coefficient at 280 nm (20).

Inhibition Assays—Enzyme activity assays using L-DOPA as a substrate were performed at 21 °C by optically following the formation of the DOPAchrome reaction product at 475 nm according to the method described previously (21). Over the time course of the experiment, linear product formation was observed in all cases. Inhibition constants were obtained by measuring values of V_{max}/K_m, corresponding to the slopes of the Michaelis-Menten plots, in the presence of at least 5 different concentrations of halide inhibitor, [I], and by using five different substrate concentrations at each [I]. The plots of V_{max}/K_m *versus* [I] appeared linear within the error of the experiment (estimated at ±10%) in all cases, allowing for an estimation of K_i^{app} from the slope and the intercept. The halide concentrations in the assay mixture were chosen both well below and above the value of the apparent inhibition constant for the halide under consideration. For the pH dependence of halide inhibition, a 75 mM phosphate, 25 mM borate instead of a 100 mM P_i buffer was used to ensure efficient buffering at all pH values used. The enzyme was stored in the form of a 5 mM P_i stock solution at pH 7.2 to prevent protein degradation during storage prior to the experiments. Enzyme was added to the assay medium directly from this stock. The reported pH values were measured on the final mixed solutions.

Preparation of Ty_{oxy}/Ty_{red}—All steps were performed in a cold chamber (4 °C) using air-saturated buffers obtained by vigorous shaking under air for at least 1 h. The pH of the buffers used was 6.80 (measured at 21 °C) throughout the procedure. A mixture containing Ty_{oxy} and Ty_{red} was prepared by the incubation of a 5 mM P_i solution containing the protein (~5 μM) with 0.5 mM hydroxylamine resulting in complete reduction of Ty_{met} to Ty_{red}. The binding of oxygen from the air-saturated reaction buffer (~ 0.27 mM O_2) to Ty_{red} results in the formation of a mixture of ~95% Ty_{oxy} and ~5% Ty_{red} (K_d = 17 μM).[2] The reaction mixture was applied immediately to a small column containing ~0.5 ml of CM-Sepharose column material, which had previously been equilibrated with 5 mM P_i buffer. To remove excess hydroxylamine, the column was washed extensively with the equilibration buffer after which the protein was eluted with 100 mM P_i buffer in a volume varying between 2 and 5 ml. Because the Ty_{oxy} protein is unstable,[2] the protein solution was made immediately prior to the experiments.

Halide Titration of Ty_{oxy}—A solution of ~95% Ty_{oxy} and ~5% Ty_{red} (1 ml in a sealed cuvette; typically 3 μM total concentration) in 100 mM air-saturated P_i buffer at pH 6.80 and 4 °C was allowed to equilibrate to 21 °C after which halide was added in 5–20 μl volume steps from concentrated stock solutions of 2.00 M F^-, 5.00 M Cl^-, 1.00 M Br^-, or 100 mM I^- made up in the assay buffer. Absorption changes were measured at 345 nm.

NMR Spectroscopy—NMR Ty_{met} samples (~0.6 mM in 100 mM NaP_i at pH 6.80) were prepared as described previously (14). Exogenous ligands were added to the samples from concentrated stock solutions prepared by using the same buffer as for the measurement. The pH of the NMR samples was varied by adding small aliquots of either dilute NaOH or 100 mM H_3PO_4 under continuous mixing and monitoring of the pH. ^{1}H spectra were recorded at 600 MHz using a Bruker DMX-600 spectrometer with the super-WEFT pulse sequence (22). Depending on the required signal-to-noise ratio, 4,000–128,000 FIDs were recorded and Fourier-transformed using a 60 Hz exponential window function (LB); the base line was corrected using software provided by Bruker.

[2] A. W. J. W. Tepper, L. Bubacco, and G. W. Canters, unpublished data.

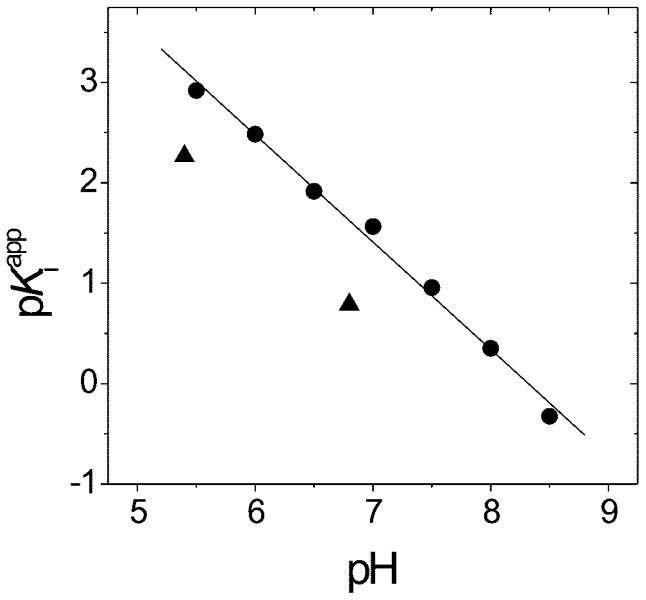

FIG. 1. **The pH dependence of the apparent value of the fluoride (●) and chloride (▲) inhibition constants using L-DOPA as the substrate.** Measurements were performed in a 75 mM phosphate, 25 mM borate buffer at 21 °C. The *solid line* represents a least-squares linear fit to the fluoride inhibition data using the equation $pK_I^{app} = 8.90 - 1.06 \times pH$.

One-dimensional NOEs on $Ty_{met}F$ were measured as described previously (14, 23).

RESULTS

Halide Inhibition—To characterize the effect of halides on the enzymatic activity, we performed steady-state kinetic measurements using diphenolic L-DOPA as the substrate at pH 6.80 and room temperature. In all cases, product formation linear in time was observed, and the dependence of the reaction rate *versus* [L-DOPA] obeyed Michaelis-Menten type kinetics. For all halides studied, the plots of K_m/V_{max} values obtained from the slope of the Michaelis-Menten plots *versus* $[X^-]$ showed the linear dependence (see Supplemental Material), indicating that the binding of a single halide ion is responsible for the inhibition (24). The fluoride and chloride inhibitions appeared competitive, whereas iodide and bromide inhibit through an apparent noncompetitive mechanism (supporting information). The order of strength of inhibition is $I^- > F^- \gg Cl^- > Br^-$ with apparent inhibition constants of 3.8 mM, 11 mM, 0.16 M, and 0.23 M, respectively.

We studied the pH dependence of fluoride inhibition. The fluoride inhibition appeared very sensitive to the pH, as depicted in Fig. 1; in the plot of pK_{I,F^-}^{app} *versus* pH, an approximately linear dependence is observed. A linear least-squares fit to the data yields the relationship $pK_{I,F^-}^{app} = 8.9 - 1.06 \times pH$. These data can be explained by adopting Scheme 2,

$$Ty \underset{K_a}{\overset{H^+}{\rightleftharpoons}} Ty^* \underset{K_{i,F^-}}{\overset{F^-}{\rightleftharpoons}} TyF$$

SCHEME 2

where Ty* denotes the acidic form of the enzyme, which is capable of binding fluoride. Assuming that $Ty_{met}F$ is catalytically inactive, the equation relating the pH to the observed inhibition constant becomes

$$K_{i,F^-}^{app} = K_{i,F^-}\left(\frac{K_a}{[H^+]}+1\right) \qquad \text{(Eq. 1)}$$

In the region where $[H^+] \ll K_a$, Equation 1 may be simplified to become

$$pK_{i,F^-}^{app} = -\log(K_a K_{i,F^-}) - pH = (pK_{i,F^-} + pK_a) - pH \qquad \text{(Eq. 2)}$$

and pK_{I,F^-}^{app} becomes directly proportional to the pH. The data in Fig. 1 exhibit no curvature down to pH 5.5, indicating, according to Equation 1, that the pK_a value is <5.5. Measurements at the lower pH values were prohibited because of complications arising from the less efficient chemical disproportionation of the enzymatic product DOPAquinone into L-DOPA and DOPAchrome (25), the latter being the measured substance, as well as the intrinsic instability of the enzyme at pH values lower than ~5. We chose not to measure above pH 8.5 because of the very high fluoride concentrations (hence ionic strengths) required to accurately measure pK_{I,F^-}^{app} values. The chloride inhibition constant was determined at both pH 6.80 and 5.40 (see Fig. 1), showing that a similar pH dependence occurs for the inhibition by chloride ion. For a comparison with ^1H NMR data (see below), we also determined the apparent inhibition constant for fluoride at 4 °C and pH 6.80, which amounts to 3.4 mM ($pK_{I,F^-}^{app} = 2.5$).

Paramagnetic ^1H NMR—Fig. 2 shows the 600 MHz ^1H NMR spectra of native *S. antibioticus* Ty_{met} (*panel A*) and Ty_{met} in the presence of 0.2 M fluoride (*panel B*; $Ty_{met}F$), 0.5 M chloride (*panel C*; $Ty_{met}Cl$), and 0.5 M bromide (*panel D*; $Ty_{met}Br$) between 55 and 10 ppm. All investigated species displayed well resolved paramagnetically shifted NMR signals. No paramagnetically shifted signals could be detected in the up-field or in the >55 ppm down-field region in all cases. We did not attempt to detect paramagnetically affected signals under the diamagnetic envelope. The addition of iodide to a final concentration of 0.2 M to a sample of Ty_{met} did not lead to changes in the ^1H NMR spectrum apart from a significant loss of signal intensity, possibly indicating that iodide ion reduces the copper ions under the conditions of the experiment or that it destabilizes the Ty_{met} protein. The observed changes upon the addition of halide cannot be assigned to the increase in ionic strength, as the addition of 0.25 M Na_2SO_4 to a sample of native Ty_{met} in 100 mM P_i at pH 6.8 did not affect the paramagnetic part of the spectrum. The spectra of native Ty_{met} and $Ty_{met}Cl$ have been discussed previously (14).

The spectra of the three halide-bound derivatives each displayed several well resolved paramagnetically shifted signals. The shift pattern is rather similar for the chloride- and bromide-bound species, whereas the signal distribution of the $Ty_{met}F$ species appears to be quite different. Yet, in each halide-bound derivative, six sharp signals together with several broader, partially overlapping signals can be distinguished. For $Ty_{met}Cl$, the hyperfine shifted resonances could be assigned (14) based on H_2O/D_2O exchange experiments, intra-residue NOE patterns, and T_1 relaxation data. The total signal intensity in the 10–50 ppm range appeared compatible with what can be expected for the combined signals of six histidines (14). The sharp solvent-exchangeable signals, marked with *asterisks* in Fig. 2, were assigned to the histidine Nδ protons, whereas the broader signals could be assigned to the His-Cϵ and His-Cδ protons of the coordinating histidines. The latter are closer to the copper and therefore experience stronger paramagnetic relaxation and hence more broadening compared with the Nδ protons. Furthermore, the observed NOE patterns allowed us to couple each of the six sharp Nδ proton signals with a broader Cϵ signal, thereby identifying each histidine residue in the six-coordinate ligand sphere of the Cu_2 site. Because the observed signal shift pattern is quite different for the $Ty_{met}Cl$ than for the $Ty_{met}F$ species, we repeated the assignment procedure for $Ty_{met}F$. Fig. 2*B* shows the spectrum recorded in D_2O.

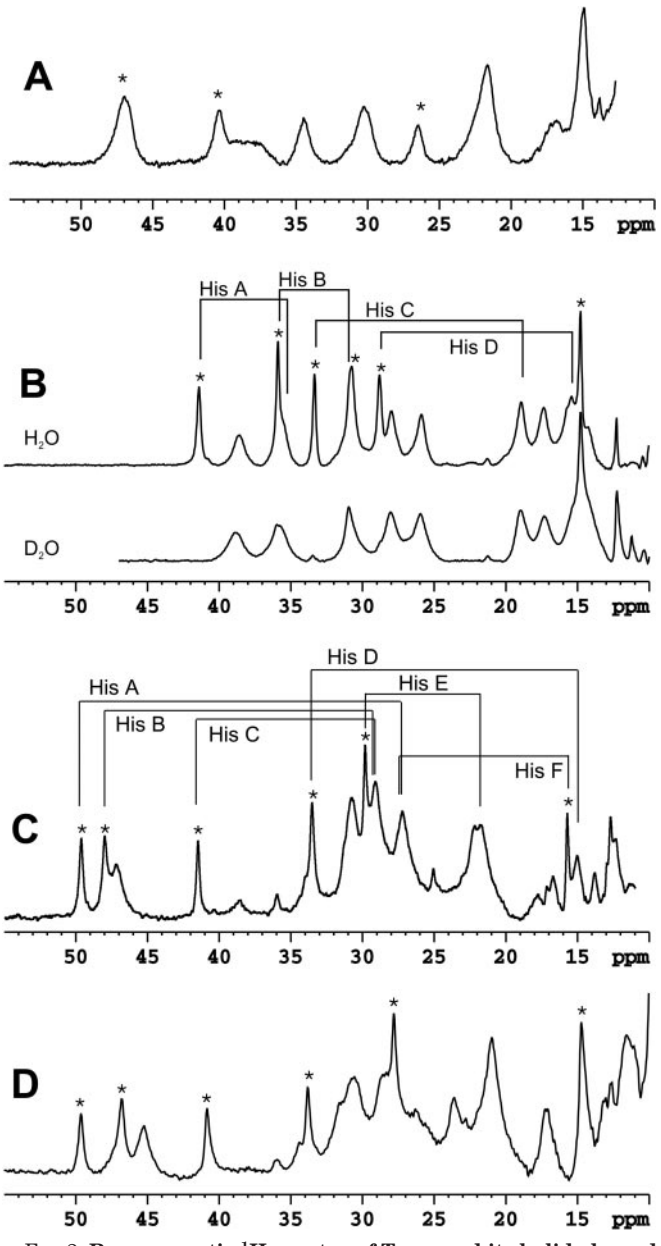

FIG. 2. **Paramagnetic ^{1}H spectra of Ty_{met} and its halide-bound derivatives.** All spectra were recorded at a 600 MHz resonance frequency and 4 °C using the super-WEFT pulse sequence. All samples were buffered with 100 mM P_i at pH 6.80. Solvent-exchangeable signals assigned to coordinating His Nδ protons are labeled with an *asterisk*. *A*, native Ty_{met}. *B*, Ty_{met} in the presence of 0.20 M fluoride recorded in H_2O (*top*) or D_2O (*bottom*) illustrating proton exchangeability. *C* and *D*, Ty_{met} in the presence of 0.50 M chloride (*C*) or 0.75 M bromide (*D*). In *B* and *C*, the drawn lines represent NOE connectivity detected between His Nδ and Cϵ protons. The *His A–His D* labels in *B* do not correspond to the *His A–His F* labels in *C*.

It can be observed that five of the six sharp signals are readily solvent-exchangeable similar to what is observed for the chloride-bound species (14). The detection of NOE couplings between the paramagnetically shifted ^{1}H signals in $Ty_{met}F$ is complicated due to both the relatively fast $Ty_{met}F$ T_1 proton relaxation[2] and the presence of considerable signal overlap, for example for the signal at 31 ppm that is composed of both a sharp and a broad signal. Yet, we were able to establish four NOE connectivities as indicated in Fig. 2. The expected NOE couplings from the sharp signals at 31.0 and 14.8 ppm to broader signals remain undetectable thus far. Further assignments must await the outcome of additional experimentation.

pH Titrations of $Ty_{met}F$ and $Ty_{met}Cl$—The NMR spectra of samples of ~0.5 mM Ty_{met} containing 0.2 M fluoride or 0.5 M chloride are clearly pH-dependent, as shown in Fig. 3 for fluoride ion. The observed effects are fully reversible. For both of the halide-bound species similar titration behavior is observed. The spectra of Ty_{met} recorded in the presence of fluoride or chloride at pH 9.6 superimpose well on the spectrum of native Ty_{met} at pH 6.8 (Fig. 2*A*), showing that the protein reverts to native Ty_{met} when the pH is increased. No signal broadening effects or shifts are observed over the whole titration range for all observable signals for both species, showing that the halide exchange process is slow on the NMR time scale in both cases. As a consequence, the signals of native Ty_{met} and $Ty_{met}F$ or $Ty_{met}Cl$ can be followed independently. The midpoint of the titration occurs at a pH of ~8.2 for $Ty_{met}F$ ($[F^-] = 0.2$ M) and at pH ~7.8 For $Ty_{met}Cl$ ($[Cl^-] = 0.5$ M). We did not quantify signal intensities because partial protein degradation at the extremes of the pH values used prevented accurate comparison between individual spectra. A quantitative analysis of the pH dependence of fluoride binding is presented below. A pH titration of native Ty_{met} toward the lower pH values was unsuccessful because of irreversible protein degradation leading to a rapid loss of signal intensity.

Fluoride Titrations of Native Ty_{met} at Two pH Values—The observed pH dependence of fluoride binding and inhibition prompted us to investigate fluoride binding at fixed pH. More specifically, we performed a titration of native Ty_{met} with fluoride at two pH values (pH 7.06, $[F^-]$ 0–38 mM, and pH 8.03, $[F^-]$ 0–375 mM). These pH values were chosen in the region of maximal stability of the protein to prevent protein degradation during the experiment. The observed titration behavior is the reverse of that observed in the pH titration described above (Fig. 3), in agreement with a two-state model where both species are in slow exchange on the NMR time scale. There is no indication of the occurrence of intermediates during the titration, in agreement with the binding of a single fluoride ion. The relative amounts of native Ty_{met} and $Ty_{met}F$ were determined by measuring peak heights. For native Ty_{met}, this was carried out on the isolated signals at 47.2 and 22.0 ppm where there is no overlap with signals originating from the fluoride-bound species. The relative amount of $Ty_{met}F$ was determined by measuring the intensity of the sharp Nδ proton signals 28.8, 33.3, 35.9, and 41.4 ppm. The intensity of the signals were normalized and then fitted to the general equation for two-state binding under the conditions that the ligand is in large excess over the enzyme,

$$\frac{I_{obs,A}}{I_{max,A}} = 1 - \frac{[F^-]}{K_d^{app} + [F^-]} \quad \text{(Eq. 3)}$$

$$\frac{I_{obs,F}}{I_{max,F}} = \frac{[F^-]}{K_d^{app} + [F^-]} \quad \text{(Eq. 4)}$$

where $I_{obs,F}$ and $I_{obs,A}$ represent the observed signal intensities of $Ty_{met}F$ and native Ty_{met}, respectively. K_d^{app} represents the apparent value for the dissociation constant of the fluoride-bound complex, $I_{max,A}$, the signal intensity of the native species at zero $[F^-]$ and $I_{max,F}$ the $Ty_{met}F$ signal intensity at $[F^-] \gg K_d^{app}$. For each of the two titration experiments, K_d^{app} was set as a shared parameter between the $I_{obs,F}$ and $I_{obs,A}$ *versus* $[F^-]$ data sets, resulting in a single value for K_d^{app}, $I_{max,A}$, and $I_{max,F}$ at each pH. At both pH values, good fits were obtained as depicted in Fig. 4, *left panel* (pH 7.06) and *right panel* (pH 8.03). The values obtained for K_d^{app} amounted to 5.8 and 51 mM at pH 7.06 and 8.03 with corresponding pK_d^{app} values of 2.24 and 1.29, respectively. The difference in the pK_d^{app} values is 0.94, comparing well with the difference in the pH values of the exper-

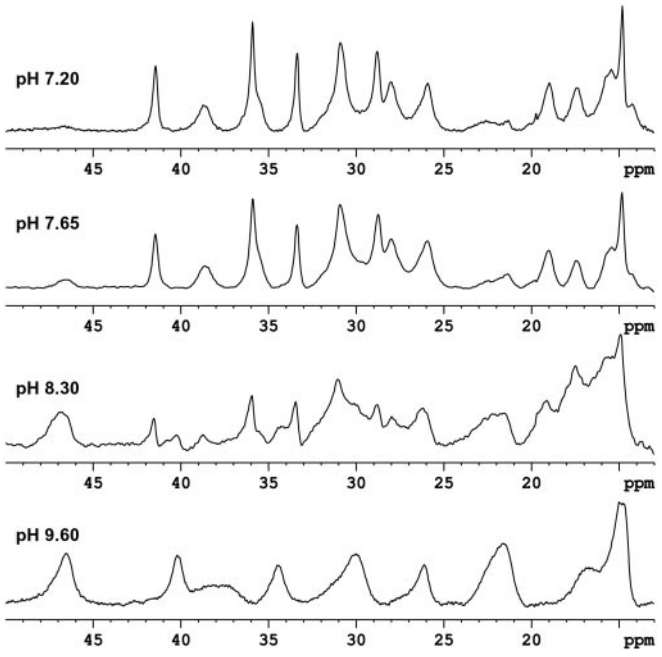

FIG. 3. **pH titration of $Ty_{met}F$ illustrating the displacement of fluoride from the Ty_{met} enzyme at high pH (4 of 6 titration steps are shown).** At low pH, Ty_{met} occurs in the fluoride-bound form (see Fig. 2*B*) and reverts to the native species (Fig. 2*A*) upon an increase in pH. Similar behavior is observed with chloride. The conditions were 0.6 mM Ty_{met}, 200 mM F^-, 100 mM P_i, pH 6.80, and 4 °C.

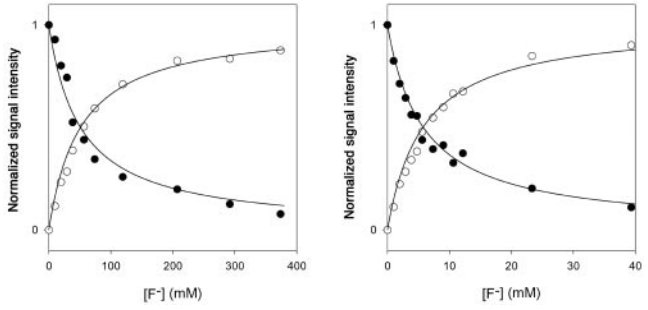

FIG. 4. **Normalized paramagnetic ^1H signal intensities of native Ty_{met} (●) and $Ty_{met}F$ (○) as a function of [F^-] at pH 7.06 (*left*) and pH 8.03 (*right*).** The *solid lines* represent best fits to Equations 3 and 4 yielding fluoride dissociation constants of 5.8 and 51 mM at pH 7.06 and 8.03, respectively. Measurements were made with 0.6 mM Ty_{met} in 100 mM P_i at 4 °C using the super-WEFT pulse sequence.

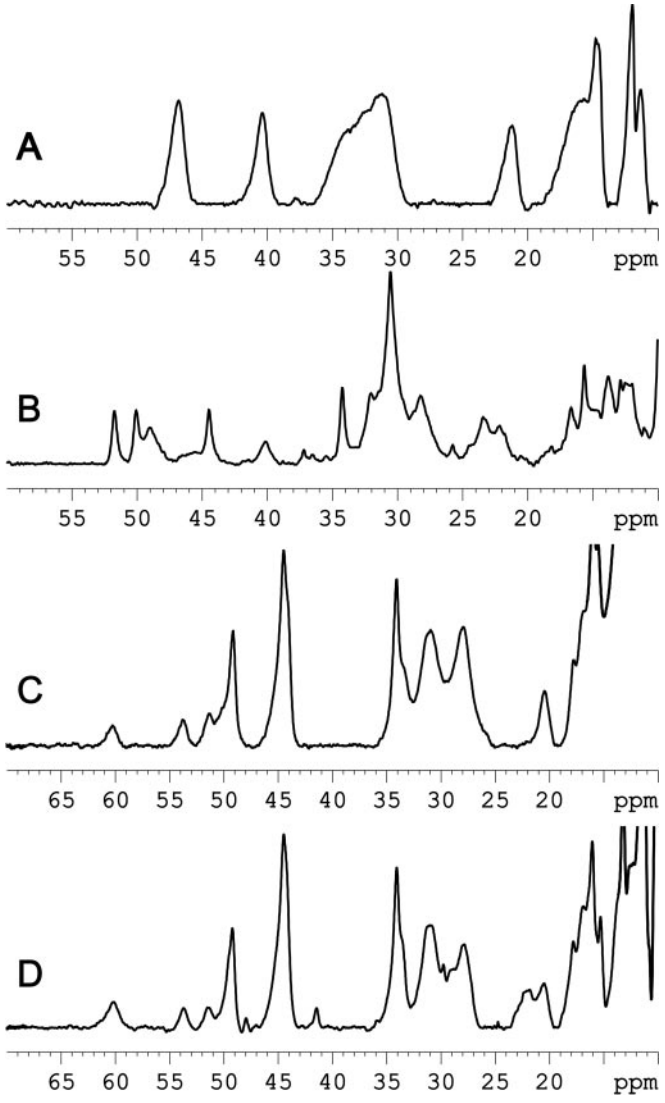

FIG. 5. **Paramagnetic ^1H spectra of various complexes of Ty_{met}.** Experimental conditions were as described in the legend for Fig. 2. *A*, Ty_{met} + 1.4 mM *p*-nitrophenol. *B*, Ty_{met} + 0.5 M Cl^- + 8.4 mM *p*-nitrophenol; *C*, Ty_{met} + 1.0 mM Kojic acid; *D*, Ty_{met} + 0.5 M Cl^- + 1.0 mM Kojic acid. The results show that *p*-nitrophenol interacts with both Ty_{met} (compare *A* with Fig. 2*A*) and $Ty_{met}Cl$ (compare *B* with Fig. 2*C*), whereas the chloride ion is displaced from the enzyme by Kojic acid (compare *C* and *D*). Signal assignment studies are under way.

iments (0.97). This shows that the fluoride dissociation constant, like the fluoride inhibition constant (Fig. 1), is inversely proportional to the proton concentration in the pH range of 7 to 8, and it explains why the halide is displaced from $Ty_{met}X$ at fixed [X^-] upon increasing the pH (see Fig. 3).

Halide Displacement Studies—To obtain a better insight into the mode of halide and inhibitor binding in the oxidized [Cu(II)-Cu(II)] species, we recorded ^1H NMR spectra of ~0.5 mM native Ty_{met} and $Ty_{met}Cl$ ([Cl^-] = 0.5 M) in the presence of the bidentate inhibitor Kojic acid or the monodentate ligand *p*-nitrophenol. The resulting spectra are represented in Fig. 5. It appears that the spectra of Ty_{met} + Kojic acid recorded in the absence and presence of chloride are nearly identical (Fig. 5, *C* and *D*), indicating that Kojic acid displaces chloride from the active site. The small differences between the spectra can be explained by assuming that there is still a small fraction of $Ty_{met}Cl$ present in solution (compare Fig. 2*C* with Fig. 5*D*). Analogous behavior is observed with the bidentate carboxylic acid inhibitor *p*-toluic acid (not shown). The situation is different with the monodentate phenolic substrate analogue *p*-nitrophenol, where the spectrum is clearly dependent on the presence of chloride (Fig. 5, *A* and *B*). Interestingly, in the absence of chloride, the spectrum of Ty_{met} containing *p*-nitrophenol shows some similarities with that of the native enzyme (compare Figs. 2*A* with 5*A*) in that large changes occur for the signals only at 34.5, 30.2, and 26.5 ppm in the native species. When chloride is added to a sample containing the Ty_{met} enzyme and *p*-nitrophenol, the spectrum changes significantly, as shown in Fig. 5*B*, and is clearly different from the spectrum of $Ty_{met}Cl$ (compare peak positions with Fig. 2*C*). Significantly more *p*-nitrophenol is required to observe changes in the spectrum when chloride is present than in the absence of chloride. The obtained spectra were not dependent on the order in which *p*-nitrophenol and chloride were added to the Ty_{met} sample. These data firmly demonstrate that both *p*-nitrophenol and chloride can bind simultaneously to the Ty_{met} protein, thereby forming a ternary complex.

Displacement of Ty-bound Oxygen by Halide—The effects of halide on the $Ty_{oxy} \rightleftharpoons Ty_{red} + O_2$ equilibrium were studied by halide titration of a mixture of ~95% Ty_{oxy} and ~5% Ty_{red} in an

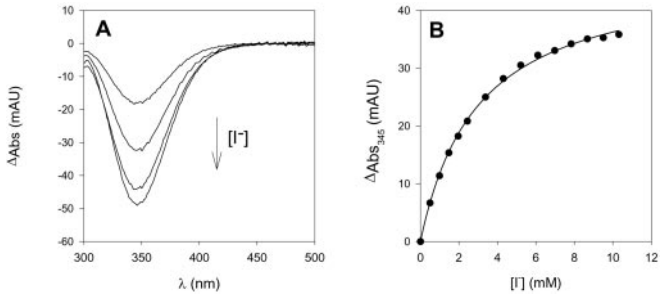

FIG. 6. **Displacement of molecular oxygen from Ty_{oxy} by iodide.** *A*, difference absorption spectra obtained by adding an increasing amount of I^- to a sample containing ~95% Ty_{oxy} and ~5% Ty_{red} (~3 μM total concentration) in 100 mM P_i buffer at pH 6.80 and 21 °C. *B*, ΔAbs_{345} *versus* [I^-]. The *solid line* represents the best fit to the data ($K_d^{app}{}_{,I^-}$ = 3.0 mM). Bromide ($K_d^{app}{}_{,Br^-}$ = 50 mM) and chloride ($K_d^{app}{}_{,Cl^-}$ > 0.5 M) exert similar behaviors, whereas no significant changes in the Ty_{oxy} spectrum are observed when fluoride is used as the titrant (not shown).

air-saturated buffer at 21 °C ([O_2] = 0.27 mM) and pH 6.80 by following the LMCT transition at 345 nm associated with Ty_{oxy}. The addition of fluoride up to 200 mM did not lead to significant changes in the Ty_{oxy} spectrum, indicating that this ion does not interact with either Ty_{oxy} or Ty_{red}. This was different for Cl^-, Br^-, and I^-, in which a decrease in the Ty_{oxy} LMCT intensity was observed, as shown in Fig. 6 for iodide ion. The observed changes are reversible. The titration data obtained for Br^- and I^- could be fitted accurately to a function of the type of Equation 4, yielding apparent dissociation constants of 50 and 3.0 mM, respectively. The Cl^- titration data showed little saturation up to 1 M of chloride and only allowed estimation of a lower limit for K_d^{app} of ~0.5 M. All titration data are easily explained by assuming in accordance with Scheme 3 that halide is in competition with molecular oxygen for binding to Ty_{red}.

$$Ty_{oxy} \underset{O_2}{\overset{K_{O_2}}{\rightleftharpoons}} Ty_{red} \underset{K_{X^-}}{\overset{X^-}{\rightleftharpoons}} Ty_{red}X^-$$

SCHEME 3

The apparent dissociation constant for halide, K_X^{app}, is dependent on the oxygen concentration in the sample, according to Equation 5,

$$K_X^{app} = K_{X^-} \times \frac{(K_{O_2} + [O_2])}{K_{O_2}} \qquad \text{(Eq. 5)}$$

where K_{X^-} denotes the dissociation constant for the halide-Ty_{red} complex and K_{O_2} denotes the oxygen dissociation constant of Ty_{oxy}. By using a value for the oxygen equilibrium dissociation constant of 17 μM,[2] the true binding constants for bromide and iodide can be calculated, amounting to 3.4 and 0.20 mM, respectively.

DISCUSSION

We have studied the mechanism of halide inhibition in detail through complementary kinetic, optical equilibrium titration, and paramagnetic ^{1}H NMR studies. It appears that all halides act as inhibitors in the conversion of diphenolic L-DOPA, as found before with Ty from other organisms (16–18). The determined inhibition constants follow the order $I^- < F^- \ll Cl^- < Br^-$, whereas different orders have been found for other Ty (16, 17) (see below). With respect to the L-DOPA conversion, the inhibition mechanism is purely competitive for fluoride and chloride, whereas iodide and bromide apparently inhibit non-competitively. Our results show that this can be explained by invoking a different interaction of different halides with the oxidized Ty_{met} and reduced Ty_{red} enzyme species. These interactions will be discussed separately. We will first consider the interaction of halides with the Ty_{met} species, which is EPR silent, shows no strong UV-visible absorption bands, and therefore is not easily studied by spectroscopic techniques other than paramagnetic NMR.

The Interaction of Halide Ion with Ty_{met}—All of the data collected are in agreement with the concept that halides interact directly with the dinuclear type-3 copper active center, as previously proposed for other tyrosinases (16–18) and hemocyanins (11, 26, 27). This is exemplified by the great changes in the paramagnetic ^{1}H NMR that occur when halide ($X^- = F^-$, Cl^-, Br^-) is added to native Ty_{met} (Fig. 2), showing that the electronic structure of the dinuclear site is strongly perturbed upon halide binding. Changes occur over the whole spectrum when halide is added to native Ty_{met}, both in terms of signal distribution and line widths, indicating alterations in the spin distribution over the ligands and in the relaxation properties of the coupled system (59). Through a detailed assignment procedure it was shown previously that the 2 copper ions in $Ty_{met}Cl$ are coordinated by 6 His residues through their Nϵ atoms (14), similar to the coordination mode found in other type-3 copper proteins for which a structure has been reported (28–31). The clear similarities between the $Ty_{met}Cl$ (Fig. 2*C*) and $Ty_{met}Br$ (Fig. 2*D*) spectra indicate that the typical type-3 coordination mode also occurs in $Ty_{met}Br$. Because the signal distribution appeared quite different in $Ty_{met}F$ (Fig. 2*B*), the assignment procedure was repeated for this species, leading us to conclude that the typical type-3 coordination is maintained in $Ty_{met}F$ as well. If the halide ion coordinates to copper in the active site, it must therefore bind to a position that is not occupied by a histidine in the absence of halide. We propose that halides (F^-, Cl^-, Br^-) bridge the two copper ions in the active site. Indeed, halide bridging is commonly found in dinuclear copper model complexes (*e.g.* see Refs. 32–39), and it has also been proposed for both met and half-met hemocyanin (11, 26, 27, 60). We note that exchange of the Cu_2 bridging ligand would affect the magnitude of antiferromagnetic coupling (*i.e.* $-2J$) between both copper ions (33, 38, 39) and the electron spin distribution over the ligands of both copper ions, thereby affecting the contact coupling constant A for each signal. Because the hyperfine shifts are a function of both $-2J$ and A (14), it is expected that the shifts for the paramagnetically affected ^{1}H NMR signals are all dependent on the nature of the Cu_2 bridging ligand. These considerations are consistent with the observed qualitative differences in the paramagnetic ^{1}H spectra of the different halide-bound Ty_{met} species. The variations in the nuclear relaxation rates and coupling constants and the magnitude of $-2J$ between the three $Ty_{met}X$ species will be described elsewhere.

It appears that the apparent fluoride and chloride inhibition constants (Fig. 1) as well as the dissociation constants for fluoride and chloride binding to native Ty_{met} (Figs. 3 and 4) are pH-dependent. The simplest way to explain these data is by using Scheme 2, where the halide binding is under the control of a single protein-derived acid/base equilibrium and where halide binds only to the acidic form of the enzyme, rendering a kinetically inactive complex. The data presented allow us to conclude only that the pK_a value of this acid/base is less than 5.5. A pH-dependent anion binding has also been observed for met hemocyanin (40) and several dinuclear copper model complexes (41, 42). To explain the pH dependence of the inhibition of Ty by halides, it has been suggested previously that a coordinating His residue dissociates from 1 copper at low pH, thereby providing a binding site for halide ion (16–18). Our results clearly demonstrate that this is not the case for bacte-

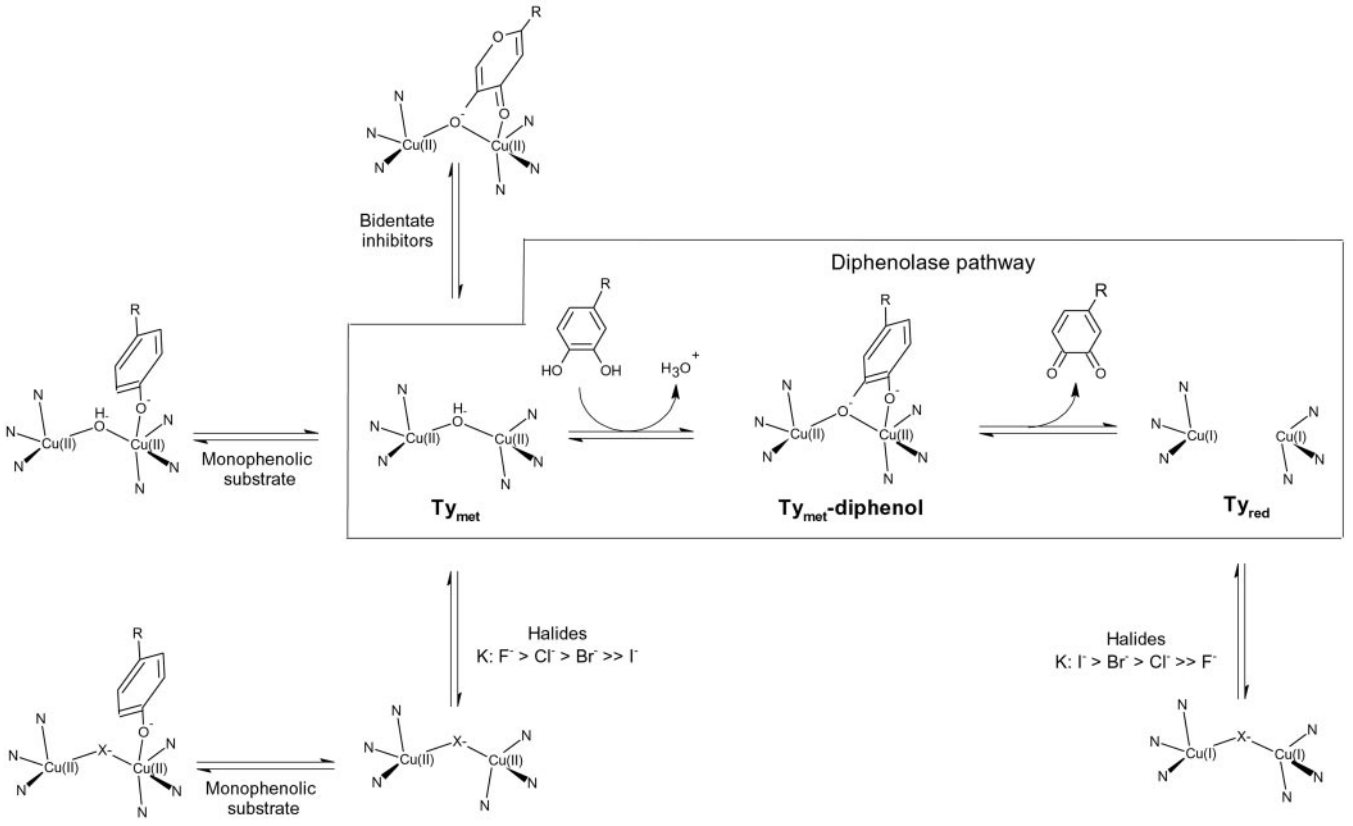

SCHEME 4. **Model of inhibitor action and the reaction of diphenols with Ty$_{met}$.** The Ty$_{met}$ diphenolase reaction is represented within the *outlined area*. Species outside of this region all represent inhibited complexes. The orientation of aromatic ligands is drawn corresponding to the structure reported for phenylthiourea-bound catechol oxidase (29). The bridging mode of halides in Ty$_{red}$ is drawn as presumed. See "Discussion" for details.

rial Ty$_{met}$. The observed pH dependence of halide binding might originate from the protonation or direct dissociation of the hydroxide molecule that bridges the two copper ions in the native Ty$_{met}$ active site at low pH, leaving the bridging position vacant and accessible for halides to bind. A pH-dependent dissociation of Cu_2 bridging hydroxide (42–45), as well as the replacement of bridging hydroxide by anions (42, 45, 46), has been observed for a number of Cu_2 model complexes. The presence of a hydroxide or water molecule at an equatorial Cu^{2+} coordination position and its displacement by exogenous ligands have been demonstrated unequivocally for *S. antibioticus* Ty$_{half\text{-}met}$ by means of pulsed EPR spectroscopy (13). The kinetics of fluoride binding, and its pH dependence are currently under investigation.

The Interaction of Halide with the Reduced [Cu(I)-Cu(I)] Enzyme, Ty$_{red}$—The Ty$_{oxy}$ titration data (Fig. 6) show that adding halide (Cl^-, Br^-, I^-) causes a decrease in the optical absorption at 345 nm associated with Ty$_{oxy}$, whereas this effect is not seen when fluoride is used as the titrant, not even when fluoride concentrations (200 mM) much higher than the apparent inhibition constant at pH 6.80 (11.8 mM) are used. The apparent dissociation constants determined at pH 6.80 decrease as we go down the halide group (K_d, $I^- < Br^- < Cl^- \ll F^-$). Although an allosteric effect of halide binding on the oxygen binding affinity cannot be excluded, the data can be interpreted more easily by assuming that halide is in competition with molecular oxygen for binding to Ty$_{red}$ according to Scheme 3. This interpretation is in line with the noncompetitive inhibition with respect to [L-DOPA] as observed for iodide in the conversion of diphenols. Noncompetitive inhibition means that inhibitor and substrate do not combine with the same enzyme form, which is indeed the case when iodide only binds to Ty$_{red}$, according to Scheme 1.

Correlations between the Inhibition and the Nature of the Halide Ion—At pH 6.80, the inhibition strengths follow the order $I^- > F^- \gg Cl^- > Br^-$. In an earlier study on Ty halide inhibition (17), different orders in halide inhibition strength were found for different tyrosinases (frog epidermis Ty, $I^- > Br^- > Cl^- \gg F^-$; mushroom Ty, $F^- > I^- > Cl^- > Br^-$; mouse melanoma Ty, $F^- > Cl^- \gg Br^- > F^-$). These differences in inhibition strength have been explained mainly by relating the anion size to the accessibility to the active site. Our results show that such an explanation may be too simple. It appears that the halide inhibition is a combination of the interaction with the oxidized protein, giving rise to competitive inhibition in the conversion of L-DOPA, and the interaction with the reduced protein Ty$_{red}$, giving rise to noncompetitive inhibition. The results show that iodide interacts solely with the reduced protein, as apparent from the lack of changes in the paramagnetic ^1H spectra of Ty$_{met}$ upon addition of 0.2 M iodide ($> 50 \times K_{i,I}^{app}$) and the good agreement between the inhibition constant of iodide (3.5 mM) and the apparent dissociation constant for binding to Ty$_{red}$ (3.0 mM). In contrast, the oxidized Ty$_{met}$ species seems to be the primary site of interaction with the small F^- ion, as no evidence of binding to either Ty$_{oxy}$ or Ty$_{red}$ was obtained, whereas the apparent fluoride inhibition constant determined at 4 °C and pH 6.80 (3.4 mM; extrapolating to 6.2 mM at pH 7.06 based on Equation 1) is in good agreement with the fluoride dissociation constant for Ty$_{met}$ determined using ^1H paramagnetic NMR at pH 7.06 and 4 °C (5.8 mM, Fig. 4). Chloride and bromide are intermediate cases that interact with both Ty$_{met}$ and Ty$_{red}$. Although the mechanism of inhibition is

thus different for iodide and fluoride, their K_i values are incidentally close.

Overall, the binding affinities to Ty_{met} follow the order $F^- > Cl^- > Br^- \gg I^-$, whereas the binding to Ty_{red} is the exact reverse, $I^- > Br^- > Cl^- \gg F^-$. Indeed, this is the behavior expected from simple hard/soft ligand binding rules, with the softer ligands favoring the lower oxidation state of the Cu ions. The observations are also in line with the finding that the Cu-Cu distance in reduced sweet potato catechol oxidase is greater than the distance found for the oxidized analogue (4.4 *versus* 2.9 Å) (29). This corresponds with our observation that the Ty_{met} protein seems to favor smaller anions, whereas a larger Cu-Cu distance in the Ty_{red} reduced protein would facilitate a stable binding of the larger anions like iodide. Indeed, the Cu-Cu distance has previously been shown to be the critical factor in controlling the selectivity of anion bridging in small dinuclear copper model complexes (42) where it was found that the strongest anion binding occurs for ligands that best fit between the two Cu atoms.

Halide/Inhibitor Displacement Studies—The data presented in Fig. 5 clearly show that the monophenolic substrate analogue *p*-nitrophenol binds to the oxidized Ty_{met} protein. The formed complex is kinetically a dead-end complex according to Scheme 1, which means that this is a wasteful event from a mechanistic point of view. This interaction of Ty_{met} with monophenols was proposed earlier on the basis of kinetic data (47–49) but has never been shown directly. The data further show that *p*-nitrophenol also binds to $Ty_{met}Cl$, yielding a ternary Ty_{met}-Cl^--*p*-nitrophenol complex. Apparently, the binding of the monophenolic ligand does not displace the halide ion, meaning that the monophenol probably coordinates to an axial position on one of the coppers if it is assumed that halides block the bridging position. This is in agreement with the diphenol coordination proposed for the closely related enzyme sweet potato catechol oxidase on the basis of x-ray structure data of the oxidized protein with the inhibitor phenylthiourea bound (29). Different *p*-nitrophenol-Ty_{met} complexes are presently under NMR investigation. In contrast to the monophenolic *p*-nitrophenol, inhibitors containing a hydroxyketone or carboxylate functional group clearly displace the chloride ion from the active site (Fig. 5, *C* and *D*). We interpret these results in the light of EPR studies on $Ty_{half\text{-}met}$ (13), where it was shown that bidentate ligands coordinate in a bidentate fashion to 1 copper in the active site, displacing the equatorially bound water or hydroxide that is present in the absence of exogenous ligands. The results presented here corroborate these findings and further allow us to extend the model to the diphenolase pathway, as shown in Scheme 4, where we propose that the diphenolic substrate adopts a similar coordination geometry as bidentate transition state analogues.

Concluding Remarks—Because both the pH and chloride concentration may vary strongly in biological materials, the findings presented here are relevant to biotechnological applications of Ty, such as Ty-based biosensors (*e.g.* Refs. 50–52). The current work may also have physiological implications. It has been found that the activity of Ty is higher in melanocytes from blacks than in those from whites (53, 54). This variation seems not to be caused by differences in the number of melanocytes, the Ty abundance, the Ty gene activity, or the Ty gene sequence, suggesting that the Ty activity is regulated at the molecular level (54–57). In a recent study (55), it has been suggested that this difference originates from a lower pH in Caucasian melanosomes with respect to the pH in the Black organelles, causing the Ty activity and hence the extent of pigmentation to be lower in Caucasians. The present results may provide the structural basis for this effect. For bacterial Ty, we found that the apparent chloride inhibition constant (0.16 M at pH 6.80) is in the order of physiological chloride concentrations (5–200 mM). Similar values for the apparent chloride inhibition constant have been found for other Tys (17). A decrease in pH of 1 unit leads to a 10-fold increase in the fraction of Ty that is in the inactive chloride-bound form. Depending on the $[Cl^-]/K_i^{app}$ ratio, this would correspond to a maximal 10-fold decrease in total activity, thereby providing a possible explanation of the sensitivity of Ty activity to melanosomal pH. As a final remark, we note that also the multicopper laccases are inhibited by halide ions in a complex manner (58). Here, differences in halide inhibition strength among various laccases have been proposed to originate from variations in the accessibility in the channel leading to the T2/T3 site. It may well be that these variations, as well as the apparent complexity of the halide inhibition, arise from similar phenomena as described for the current system.

Acknowledgments—We are grateful to Prof. E. Katz for supplying a copy of the pIJ703 plasmid. The technical assistance of Cees Erkelens and Ursula Kolczak with the NMR measurements is gratefully acknowledged.

REFERENCES

1. Oetting, W. S. (2000) *Pigment Cell Res.* **13,** 320–325
2. Tief, K., Schmidt, A., and Beermann, F. (1998) *Brain Res. Mol. Brain Res.* **53,** 307–310
3. Xu, Y., Stokes, A. H., Freeman, W. M., Kumer, S. C., Vogt, B. A., and Vrana, K. E. (1997) *Brain Res. Mol. Brain Res.* **45,** 159–162
4. Berman, S. B., and Hastings, T. G. (1997) *J. Neurochem.* **69,** 1185–1195
5. Berman, S. B., and Hastings, T. G. (1999) *J. Neurochem.* **73,** 1127–1137
6. Higashi, Y., Asanuma, M., Miyazaki, I., and Ogawa, N. (2000) *J. Neurochem.* **75,** 1771–1774
7. Decker, H., and Tuczek, F. (2000) *Trends Biochem. Sci.* **25,** 392–397
8. Sánchez-Ferrer, A., Rodríguez-López, J. N., García-Cánovas, F., and García-Cánovas, F. (1995) *Biochim. Biophys. Acta* **1247,** 1–1
9. Solomon, E. I., Sundaram, U. M., and Machonkin, T. E. (1996) *Chem. Rev.* **96,** 2563–2605
10. van Gelder, C. W., Flurkey, W. H., and Wichers, H. J. (1997) *Phytochemistry* **45,** 1309–1323
11. Himmelwright, R. S., Eickman, N. C., and Solomon, E. I. (1979) *Biochem. Biophys. Res. Commun.* **86,** 628–634
12. Wilcox, D. E., Porras, A. G., Hwang, Y. T., Lerch, K., Winkler, M. E., and Solomon, E. I. (1985) *J. Am. Chem. Soc.* **107,** 4015
13. van Gastel, M., Bubacco, L., Groenen, E. J., Vijgenboom, E., and Canters, G. W. (2000) *FEBS Lett.* **474,** 228–232
14. Bubacco, L., Salgado, J., Tepper, A. W., Vijgenboom, E., and Canters, G. W. (1999) *FEBS Lett.* **442,** 215–220
15. Bubacco, L., Vijgenboom, E., Gobin, C., Tepper, A. W. J. W., Salgado, J., and Canters, G. W. (2000) *J. Mol. Cat. B* **8,** 27–35
16. Martínez, J. H., Solano, F., Garcia-Borrón, J. C., Iborra, J. L., and Lozano, J. A. (1985) *Biochem. Int.* **11,** 729–738
17. Martínez, J. H., Solano, F., Peñafiel, R., Galindo, J. D., Iborra, J. L., and Lozano, J. A. (1986) *Comp. Biochem. Physiol. B* **83,** 633–636
18. Peñafiel, R., Galindo, J. D., Solano, F., Pedreño, E., Iborra, J. L., and Lozano, J. A. (1984) *Biochim. Biophys. Acta* **788,** 327–332
19. Himmelwright, R. S., Eickman, N. C., and Solomon, E. I. (1978) *Biochem. Biophys. Res. Commun.* **84,** 300–305
20. Jackman, M. P., Hajnal, A., and Lerch, K. (1991) *Biochem. J.* **274**, 707–713
21. Lerch, K., and Ettlinger, L. (1972) *Eur. J. Biochem.* **31,** 427–437
22. Inubushi, T., and Becker, E. D. (1983) *J. Magn. Reson.* **51,** 128–133
23. Calzolai, L., Gorst, C. M., Bren, K. L., Zhou, Z. H., Adams, M. W. W., and LaMar, G. N. (1997) *J. Am. Chem. Soc.* **119,** 9341–9350
24. Boyer, P. D. (1970) *The Enzymes: Kinetics and Mechanism*, 3rd Ed., Vol. 2, pp. 18–25, Academic Press, New York
25. Cánovas, F. G., García-Carmona, F., Sánchez, J. V., Pastor, J. L., and Teruel, J. A. (1982) *J. Biol. Chem.* **257,** 8738–8744
26. Eickman, N. C., Himmelwright, R. S., and Solomon, E. I. (1979) *Proc. Natl. Acad. Sci. U. S. A.* **76,** 2094–2098
27. Himmelwright, R. S., Eickman, N. C., LuBien, C. D., and Solomon, E. I. (1980) *J. Am. Chem. Soc.* **102,** 5378–5388
28. Cuff, M. E., Miller, K. I., van Holde, K. E., and Hendrickson, W. A. (1998) *J. Mol. Biol.* **278,** 855–870
29. Klabunde, T., Eicken, C., Sacchettini, J. C., and Krebs, B. (1998) *Nat. Struct. Biol.* **5,** 1084–1090
30. Magnus, K. A., Hazes, B., Ton-That, H., Bonaventura, C., Bonaventura, J., and Hol, W. G. (1994) *Proteins* **19,** 302–309
31. Volbeda, A., and Hol, W. G. (1989) *J. Mol. Biol.* **209,** 249–279
32. Amudha, P., Kandaswamy, M., Govindasamy, L., and Velmurugan, D. (1998) *Inorg. Chem.* **37,** 4486–4492
33. Amudha, P., Akilan, P., and Kandaswamy, M. (1999) *Polyhedron* **18,** 1355–1362
34. Amudha, P., Thirumavalavan, M., and Kandaswamy, M. (1999) *Polyhedron* **18,** 1363–1369
35. Malachowski, M. R., Dorsey, B. T., Parker, M. J., Adams, M. E., and Kelly, R. S. (1998) *Polyhedron* **17,** 1289–1294

36. Oshio, H., Watanabe, T., Ohto, A., Ito, T., and Masuda, H. (1996) *Inorg. Chem.* **35,** 472–479
37. Pons, J., Sanchez, F. J., Labarta, A., Casabo, J., Teixidor, F., and Caubet, A. (1993) *Inorg. Chim. Acta* **208,** 167–171
38. Rodríguez, M., Llobet, A., Corbella, M., Martell, A. E., and Reibenspies, J. (1999) *Inorg. Chem.* **38,** 2328–2334
39. Thompson, L. K., Tandon, S. S., and Manuel, M. E. (1995) *Inorg. Chem.* **34,** 2356–2366
40. Wilcox, D. E., Long, J. R., and Solomon, E. I. (1984) *J. Am. Chem. Soc.* **106,** 2186
41. Amendola, V., Bastianello, E., Fabbrizzi, L., Mangano, C., Pallavicini, P., Perotti, A., Lanfredi, A. M., and Ugozzoli, F. (2000) *Angew. Chem. Int. Ed. Engl.* **39,** 2917–2920
42. Amendola, V., Fabbrizzi, L., Mangano, C., Pallavicini, P., Poggi, A., and Taglietti, A. (2001) *Coord. Chem. Rev.* **219,** 821–837
43. Castro, I., Julve, M., Demunno, G., Bruno, G., Real, J. A., Lloret, F., and Faus, J. (1992) *J. Chem. Soc. Dalton Trans.* 1739–1744
44. Monzani, E., Quinti, L., Perotti, A., Casella, L., Gullotti, M., Randaccio, L., Geremia, S., Nardin, G., Faleschini, P., and Tabbi, G. (1998) *Inorg. Chem.* **37,** 553–562
45. Monzani, E., Battaini, G., Perotti, A., Casella, L., Gullotti, M., Santagostini, L., Nardin, G., Randaccio, L., Geremia, S., Zanello, P., and Opromolla, G. (1999) *Inorg. Chem.* **38,** 5359–5369
46. Fabbrizzi, L., Pallavicini, P., Parodi, L., and Taglietti, A. (1995) *Inorg. Chim. Acta* **238,** 5–8
47. Rodríguez-López, J. N., Tudela, J., Varón, R., García-Carmona, F., and García-Cánovas, F. (1992) *J. Biol. Chem.* **267,** 3801–3810
48. Fenoll, L. G., Rodríguez-López, J. N., García-Sevilla, F., Tudela, J., García-Ruiz, P. A., Varón, R., and García-Cánovas, F. (2000) *Eur. J. Biochem.* **267,** 5865–5878
49. Fenoll, L. G., Rodríguez-López, J. N., García-Sevilla, F., García-Ruiz, P. A., Varón, R., García-Cánovas, F., and Tudela, J. (2001) *Biochim. Biophys. Acta* **1548,** 1–22
50. Peña, N., Reviejo, A. J., and Pingarrón, J. M. (2001) *Talanta* **55,** 179–187
51. Streffer, K., Vijgenboom, E., Tepper, A. W. J. W., Makower, A., Scheller, F. W., Canters, G. W., and Wollenberger, U. (2001) *Anal. Chim. Acta* **427,** 201–210
52. Wang, B., Zhang, J., and Dong, S. (2000) *Biosens. Bioelectron.* **15,** 397–402
53. Abdel-Malek, Z., Swope, V., Collins, C., Boissy, R., Zhao, H. Q., and Nordlund, J. (1993) *J. Cell Sci.* **106,** 1323–1331
54. Iwata, M., Corn, T., Iwata, S., Everett, M. A., and Fuller, B. B. (1990) *J. Invest. Dermatol.* **95,** 9–15
55. Fuller, B. B., Spaulding, D. T., and Smith, D. R. (2001) *Exp. Cell Res.* **262,** 197–208
56. Naeyaert, J. M., Eller, M., Gordon, P. R., Park, H. Y., and Gilchrest, B. A. (1991) *Br. J. Dermatol.* **125,** 297–303
57. Iozumi, K., Hoganson, G. E., Penella, R., Everett, M. A., and Fuller, B. B. (1993) *J. Invest. Dermatol.* **100,** 806–811
58. Xu, F. (1996) *Biochemistry* **35,** 7608–7614
59. Bertini, I., and Luchinat, C. (1998) *Coord. Chem. Rev.* **170,** 283–288
60. Westmoreland, D. T., Wilcox, D. E., Baldwin, M. J., Mims, W. B., and Solomon, E. I. (1989) *J. Am. Chem. Soc.* **111,** 6106–6123

Structural Basis and Mechanism of the Inhibition of the Type-3 Copper Protein Tyrosinase from *Streptomyces antibioticus* by Halide Ions

Armand W. J. W. Tepper, Luigi Bubacco and Gerard W. Canters

J. Biol. Chem. 2002, 277:30436-30444.
doi: 10.1074/jbc.M202461200 originally published online June 4, 2002